Physicochem. Probl. Miner. Process., 62(5), 2026, 225579

http://www.journalssystem.com/ppmp

Physicochemical Problems of Mineral Processing

ISSN 1643-1049

Contribution to the valorisation of sludge from the phosphate ore processing of Djebel Onk, Algeria

Yousra Boukhamla [1], Cherif Gherbi [2], Djamel Nettour [3, 4], Mohamed Chettibi [4], Nesrine Derrardjia [1], Rachid Chaib [5], Hani Amir Aouissi [6]

[1] National Higher School of Technology and Engineering, Department of Mining Engineering, Metallurgy and Materials, Mining, Metallurgy and Materials (L3M) Laboratory, 23005, Annaba, Algeria.

[2] National Higher School Cheikh Elbachir El Ibrahimi of Kouba ENS 16000 Kouba Algiers, Algeria

[3] National Higher School of Technology and Engineering, Department of Mining Engineering, Metallurgy and Materials, 23005, Annaba, Algeria

[4] Laboratory of Mineral Processing and Environment (LAVAMINE), Badji Mokhtar - Annaba University, P. O. Box 12, 23000 Annaba, Algeria

[5] Laboratory of Transports and Environment Engineering, Department of Transport Engineering, Mentouri Brothers University Constantine 1, Constantine 25000, Algeria

[6] Environmental Research Center (CRE), Annaba 23000, Algeria

Corresponding author: y.boukhamla@etu.ensti-annaba.dz (Yousra Boukhamla)

Abstract: The beneficiation of secondary resources has become a key challenge to mitigate imbalances in the international market and reduce environmental impact. This supports the development of long-term economies. Accordingly, this study aims to contribute to the valorisation of sludge generated by the phosphate ore processing at Djebel Onk, Algeria. To achieve this objective, a suite of characterization methods was used, including X-ray fluorescence (XRF), X-ray diffraction (XRD), scanning electron microscopy (SEM), inductively coupled plasma optical emission spectrometry (ICP-OES), and Fourier transform infrared spectroscopy (FTIR). All methods confirmed that apatite is the predominant phosphate mineral in the processing sludge, associated with various gangue minerals, notably calcite, dolomite, and quartz. Rare earth elements and heavy metals were also detected, but only at trace amounts, with concentrations not exceeding international standards. Desliming reduced clay and siliceous minerals and increased the apatite content, followed by reverse flotation with different collectors and depressants. Using sulfuric acid as an apatite depressant performed poorly because the release of Ca^{2+} ions into the pulp promoted the formation of $CaHPO_4$ on the apatite surface, which hindered surfactant adsorption and thus depression. A subsequent test used sodium–potassium tartrate as the depressant together with aluminum sulfate to minimize the effect of Ca^{2+} ions, yielding a concentrate with a grade of 28.67%. This outcome meets phosphate ore specifications and helps limit environmental impacts.

Keywords: beneficiation, phosphate, sludge, characterization, flotation, environmental effect

1. Introduction

Phosphate ore is an important raw material that is neither recyclable nor renewable (Sis et al., 2003). It is generally found in nature as sedimentary deposits, such as those in Morocco, the United States, Algeria, Tunisia, and China. It also occurs in igneous and metamorphic forms, as in Brazil and South Africa (Abouzeid, 2008). Sedimentary deposits are the most abundant in the Earth's crust, accounting for approximately 80%; they mainly contain apatite group minerals, including fluorapatite [$Ca_{10}(PO_4)_6(F,OH)_2$], hydroxyapatite [$Ca_{10}(PO_4)_6(OH)_2$], carbonated hydroxyapatite [$Ca_{10}(PO_4,CO_3)_6(OH)_2$], francolite [$Ca_{10}(PO_4)_6{-}x(CO_3)x(F,OH)_2{+}x$], dahllite [$3Ca_3(PO_4)_2CaCO_3$], and collophane [$3Ca_3(PO_4)nCa(CO_3,F_2,O)xH_2O$] (Dong et al., 2021a), However, several gangue minerals

DOI: 10.37190/ppmp/225579

are associated with apatite, notably calcite, dolomite, and quartz, represented by ($CaCO_3$), ($CaMg(CO_3)_2$), and (SiO_2), respectively, along with various clays (Abouzeid, 2008; Avelar et al., 2021).

The presence of these gangue minerals is an important parameter for determining the phosphate grade (Dong et al., 2021), which is expressed as % P_2O_5 (phosphorus pentoxide), BPL (bone phosphate of lime), TPL (triphosphate of lime), or % P (phosphorus—not commonly used) (Boujlel et al., 2018). The relationship between these terms is (80% BPL = 80% TPL = 36.6% P_2O_5 = 16% P) (Abouzeid, 2008). In phosphoric acid production, a high dolomite content reduces ore quality and increases reagent consumption (Ge et al., 2023). However, in the fertilizer industry, phosphate ores must have a P_2O_5 content above 30%, a CaO/P_2O_5 ratio below 1.6, and an MgO content below 1% (Ruan et al., 2019). Nevertheless, if phosphate ores do not meet these criteria, their gangue must be removed through ore beneficiation processes to meet the high demand of the international market (Sis et al., 2003).

Furthermore, several studies have investigated the revalorization of phosphate mining waste in civil engineering to mitigate its environmental impact (Aichouri et al., 2025). These wastes have been used in the production of fired bricks (Loutou et al., 2019; Ettoumi et al., 2021), cement manufacturing (S. I. Zeghina et al., 2020; Bahhou et al., 2021), as concrete aggregates (El Machi et al., 2021), and in road construction (Amrani et al., 2019). However, these approaches primarily focus on the material reuse of such wastes without recovering the valuable phosphate fraction. Therefore, the mineralurgical upgrading of fine sludge and tailings, combined with an environmental assessment of trace elements, remains insufficiently investigated.

Algeria is considered one of the major producers of high-quality phosphate ore, with an annual production of 1,200 million tons. However, the extraction process generates various types of solid and liquid waste through two treatment methods: dry and wet processing. Approximately 20% of the daily production is discharged into the Oued (river) as sludge (Tahri et al., 2023). As a result, this exploitation has generated enormous quantities of waste (such as overburden, processing residues, and washing sludge) (Derrardjia et al., 2025), which are stored at the edges of mining sites (Li et al., 2025). This leads to the occupation of vast areas and the deterioration of aesthetic quality. In the absence of waste management legislation, these wastes can pose serious environmental risks due to their chemical characteristics, particle size, and the presence of harmful substances and reagents, such as fluoride and heavy metals (Eskanlou et al., 2024; Salhi et al., 2023). However, recent studies (Tahri et al., 2023; Salhi et al., 2023) have confirmed that these muds are very rich in P_2O_5, with concentrations reaching up to 20% P_2O_5. This represents both an economic loss and a threat of environmental degradation.

The main objective of this study is to determine a detailed characterization of phosphate sludge and its recovery through flotation, shedding light on optimal conditions for enhanced phosphate extraction from treatment plant sludge at Djebel Onk.

2. Materials and methods

2.1. Materials

The Djebel Onk mining complex, located in south-eastern Algeria at approximately 34°42′21″ N and 8°00′10″ E, 9 km south of the town of Bir El Ater and 20 km from the Algerian-Tunisian border, processes approximately 10,000 tons of phosphate ore daily with an average grade of 26.53% P_2O_5 through desliming (Salhi et al., 2023), It generates over 20% liquid waste in the form of phosphate sludge discharged into the Oued. For our research, a sample of approximately 150 dm^3 of sludge from the desliming outlet was collected over a 5-hour period when the treatment plant feed contained a mixture of black and beige phosphate.

2.2. Sample preparation

The sample was divided into two parts; the first part was decanted for 7 days to remove excess water, then dried in the oven at 105 °C for 48 hours and carefully reground. The product obtained was homogenized and divided using a riffle splitter to obtain representative slices, one of which was finely reground for chemical analysis and the other used for size distribution. The second part was deslimed using a 38 μm sieve, with the main aim of removing as much of the clay material in the sample as possible, as well as fine particles that negatively affect the separation process (Aleksandrova et al., 2022).

The product obtained is decanted, dried, and then sent for analysis to identify its chemical and mineralogical composition. The deslimed sample obtained after this treatment was selected as the feed material for all flotation experiments. Its chemical composition is presented in Table 3. This sample was used as the reference feed for comparison with the flotation products.

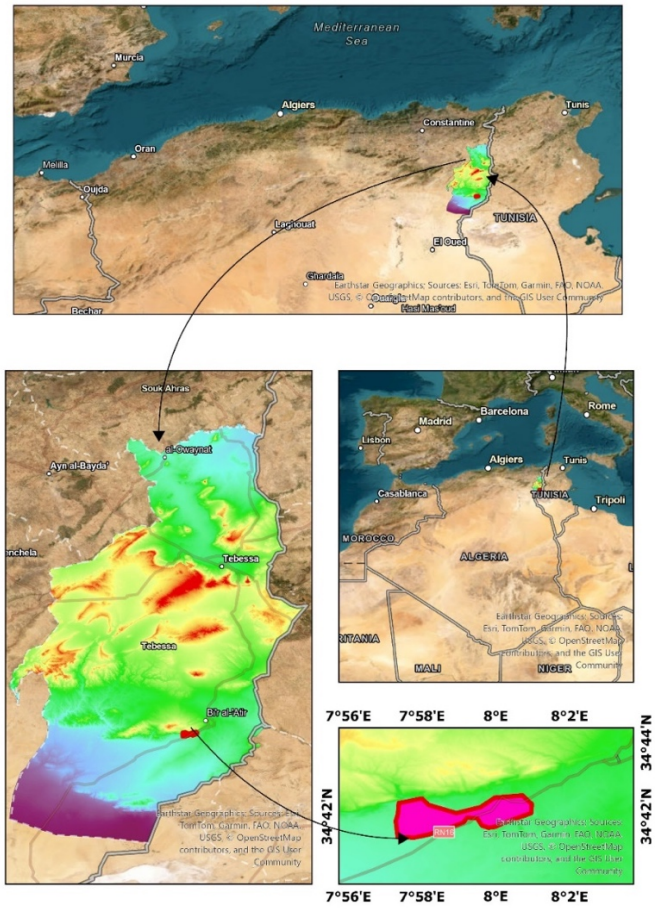

Fig. 1. Geological map and location of Djebel Onk phosphate deposits

2.3. Physico-chemical characterization

2.3.1. Particle size distribution

The particle size distribution of the raw and deslimed samples was determined by laser diffraction using a Malvern Mastersizer 2000 analyzer (measurement range: 0.1-2000 µm), with water as the dispersant medium.

2.3.2. Mineralogical analysis by X-ray diffraction (XRD)

X-ray diffraction was carried out at room temperature, to study the crystalline phases of the minerals in the samples. It was performed using a PANalytical powder diffractometer (EMPYREAN) with $\lambda_{CuK\alpha}$ radiation (λ = 1.54186 Å); the angular range was recorded between 10 and 80° (2θ) with a measurement step 0.017° and a compaction time 2s/step. Hight score plus software is used to analyse the X-ray diffraction patterns.

2.3.3. Chemical analysis

The raw and deslimed samples, as well as all flotation by-products, were collected as representative samples for chemical analysis at the Algerian phosphate company SOMIPHOS, following standard methods for phosphate ore analysis. The analyses were carried out using the SEAL Analytical Technicon auto-analyzer (AA) (made in the USA), atomic absorption spectrometry (AAS) with a Perkin Elmer precisely. AAnalyst 400 instrument, as well as the use of Bernard's method.

2.3.4. ICP-OES

The raw and deslimed sample, both finely ground were analysed by Agilent 5900 ICP-OES, the samples were digested in 15 ml of perchloric acid, the solution was boiled at 105°C on a hot plate until the reaction was completed (approximately 20 minutes), the solution was then allowed to cool, transferred to a 500 mL volumetric flask, and mixed with deionized water to the final volume. Finally, an aliquot of the diluted solution was used for ICP-OES analysis. Standard sample concentrations were measured regularly throughout the analyses to verify the calibration curve's accuracy.

2.3.5. FTIR analysis

Fourier Transform Infrared (FTIR) spectroscopy was carried out using a Thermo Scientific iS5 spectrometer, in transmission mode with potassium bromide (KBr) pellets, over a wavelength range of 4000 to 400 cm^{-1}.

2.3.6. Morphological analysis by scanning electron microscopy (SEM)

The morphological characterization of the samples was performed using scanning electron microscopy FEI QUANTA 250 (USA), equipped with an energy-dispersive X-ray spectroscopy (EDS) system. All samples were prepared to dimensions suitable for the sample chamber. Imaging was carried out at an accelerating voltage of 25 kV.

2.3.7. Chemical analysis by micro X-ray fluorescence (μXRF)

Micro X-ray fluorescence spectrometry (μXRF) was performed using a Horiba XGT-5000 energy-dispersive micro-spectrometer (EDXRF) with a spatial resolution of 100 μm, an accelerating voltage of 50 kV, and a current of 1000 μA (Nagasawa et al., 2023), The system is equipped with a digital camera, allowing clear observation of the sample during analysis.

2.3.8. Flotation separation experiment

Based on the results of the literature review (Crozier, 1992; Mohammadkhani et al., 2011), a reverse flotation process was proposed. The separation tests were carried out using a laboratory flotation machine of the Denver D-12 type, equipped with a 1.5 dm^3 cell, and operated with tap water at room temperature. The impeller rotation speed was set at 1000 rpm. For each flotation test, 300 g of sample was used, with the solid content in the pulp fixed at 21.4% for all experiments. The conditioning time was set to 10 min, while the flotation time was 3 min per stage. The separation process was conducted in two stages. The resulting products (concentrates and tailings) were dried in an oven, weighed, and then prepared for chemical analysis, mineralogical characterization by XRD, and morphological SEM analysis. The physicochemical and industrial properties of the reagents used in our study are summarized in Table 1 (El-Mofty et al., 2018; Mohammadkhani et al., 2011).

Table 1. Reagents used in the reverse flotation of phosphate sludge

Reagent	Molar mass	Chemical formula	Industry	Use
Potassium Oleate	320,56 g/mol	$C_{18}H_{33}KO_2$	Merck KGaA	Carbonate collector
Sulfuric acid	98.079 g/mol	H_2SO_4	Honeywell Fluka	Phosphate depressant
Sodium potassium tartrate	282.22 g/mol	$KNaC_4H_4O_6.4H_2O$	Sigma Aldrich	Phosphate depressant
Aluminum sulfate	342.15 g/mol	$Al_2(SO_4)_3$	Sigma Aldrich	Phosphate depressant
Hydrochloric acid	36.46 g/mol	HCl	Sigma Aldrich	pH regulator
Sodium hydroxide	39.997 g/mol	NaOH	Sigma Aldrich	pH regulator
Methylisobutylcarbinol (MIBC)	102.175 g/mol	$C_6H_{14}O$	Merck KGaA	Frother

The operating procedure was established after extensive laboratory testing. The values of the different parameters, as well as the quantities of the chemical reagents used during the flotation tests, are presented in Table 2.

Table 2. Flotation conditions for phosphate sludge

N°	Test Conditions			Flotation reagents (g/t)		
	% wt. solids	pH	flotation time (min)	Collectors	Depressants	Frother
01	21.4	4.5	3	Potassium oleate (1000)	Sulfuric acid (1000)	MIBC (10)
02	21.4	6.97	3	Potassium oleate (1000)	-	MIBC (10)
03	21.4	7.16	3	Potassium oleate (1000)	K-Na tartrate (1000) + Aluminum sulfate (500)	MIBC (10)

3. Results and discussions

3.1. Particle size distribution

Based on the laser granulometric analysis (Fig. 2), the raw sample curve shows multiple peaks, indicating a multimodal particle size distribution. A smaller peak appears around 1-2 µm, while a more prominent peak is observed between 40-70 µm, with the highest point around 50-60 µm. A slight rise is also observed for larger particle sizes, though it is less pronounced. The presence of distinct peaks suggests that this sample is composed of different particle populations and shows that the majority of the particles fall within the range of a few micrometres to about 100 micrometres. The graph also indicates three specific points on the cumulative distribution d_{10}: 5.918 µm, d_{50}: 39.299 µm, and d_{90}: 118.524 µm.

In contrast, the second curve reveals a unimodal distribution, characterized by a single, sharp, and well-defined peak centred around 80-90 µm, indicating a more uniform and coarser particle size distribution. Its cumulative distribution values are: d_{10}: 48.267 µm, d_{50}: 93.434 µm and d_{90}: 171.936 µm. Overall, these results indicate that about 50 % of the raw sample consisted of fine particles (<39 µm) which are considered detrimental to flotation efficiency. The desliming process effectively removed these fines, as evidenced by a significant increase in median particle size (d50) from 39.3 µm to 93.4 µm, resulting in a size distribution more suitable for flotation.

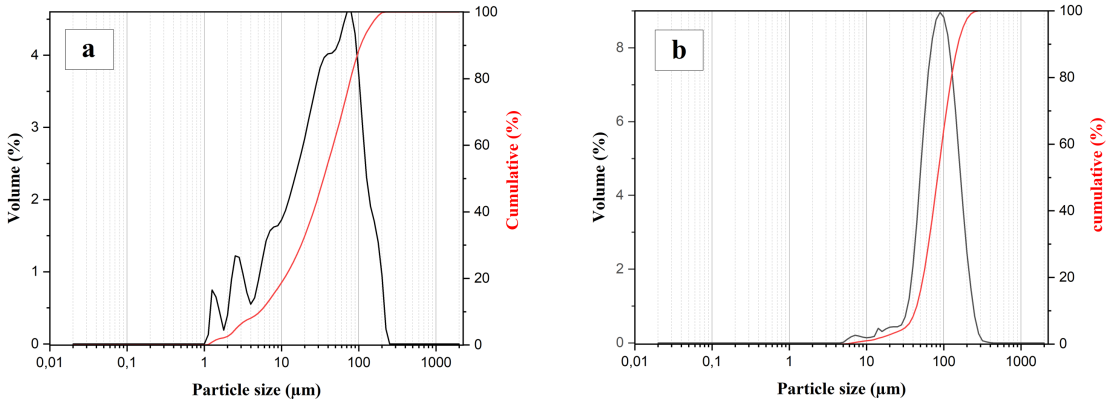

Fig. 2. Particle size distribution of: a-raw sample; b- deslimed sample

Microscopic observations of the deslimed sample (Fig. 3) reveal the presence of the main mineral constituents of the phosphate sludge. Fig. 3A shows quartz grains (QZ) associated with clay particles (CS), whereas Fig. 3B highlights phosphate pellets (PE), coprolites (CO), and dolomite grains (DO). These observations indicate that the deslimed sample consists mainly of phosphate particles associated with quartz and carbonate gangue minerals, whereas the fine clay fraction has been significantly reduced by the desliming process.

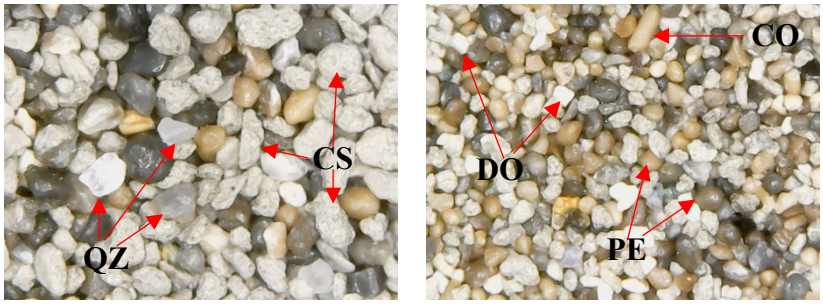

Fig. 3. Microscopic observation of the deslimed sample: (QZ) Quartz, (CS) Clays, (DO) Dolomite, (PE) Pellet, (CO) coprolite

3.2. X-ray diffraction (XRD)

X-ray diffraction was used to identify the mineralogical composition of the raw phosphate sludge sample and the sample after desliming as shown in Fig. 4, identification of the mineral phases indicates the presence of the apatite mineral in the form of carbonate hydroxyapatite [$Ca_{10}(PO_4)_3(CO_3)_3(OH)_2$], dolomite ($CaMg(CO_3)_2$) and quartz ($SiO_2$) as gangue minerals.

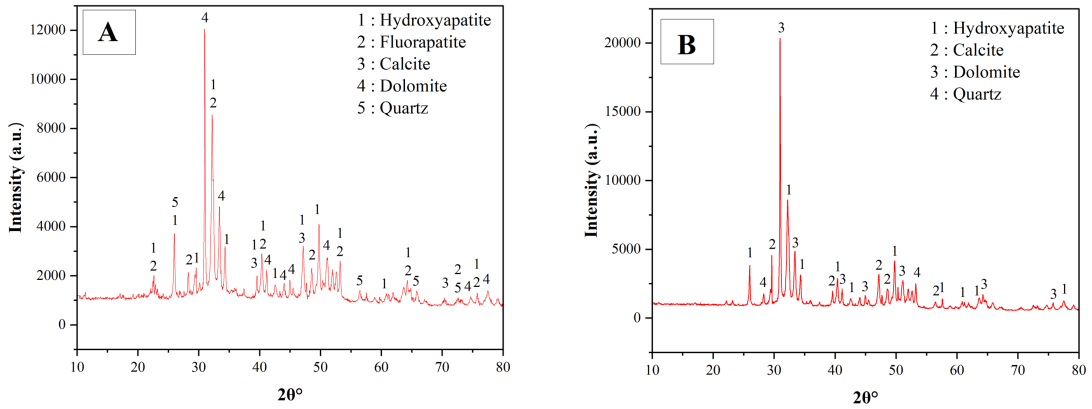

Fig. 4. Results of X-ray diffraction analysis of the raw sample (A) and deslimed sample (B)

3.3. Chemical analysis

Table 3 presents the chemical composition of the main oxides and heavy metals in the raw sample and the sample after desliming. According to these results, the P_2O_5 content was initially 23,59% and increased after desliming to approximately 27,01%, indicating that P_2O_5 is a valuable component. However, the contents of SiO_2 and MgO, considered gangue minerals, were initially 10,95% and 3,05%, respectively, and decreased after desliming to 2,30% and 2,85%, respectively. These results show that removing the fine fraction before flotation improves the quality of the sample in terms of useful mineral, thereby reducing subsequent beneficiation costs and minimizing chemical reagent consumption.

Table 3. Chemical analysis results of the raw and deslimed sample

Element	P_2O_5 %	CaO %	MgO %	SiO_2 %	H_2O %	Fe_2O_3 %	Na_2O %	K_2O %	LOI %	Cd mg.kg^{-1}	Zn mg.kg^{-1}	Cu mg.kg^{-1}	Pb mg.kg^{-1}	As mg.kg^{-1}
Raw sample	23.59	38.92	3.05	10.95	1.95	0.61	1.08	0.12	14.80	33	220	8	5	6
Deslimed sample	27.01	44.56	2.85	2.30	1.42	0.22	1.20	0.08	14.30	25	180	6	4	5.5

Numerous studies on phosphate ores have indicated the presence of heavy metals as trace elements (Boumaza et al., 2021), According to the table, it is observed that the levels of existing heavy metals decrease after desliming. Lead (Pb) concentrations in the raw and deslimed samples are 5 and 4 $mg.kg^{-1}$, respectively, which do not pose a risk since they remain below the soil standard (84 $mg.kg^{-1}$), in accordance with the World Health Organization's human health protection guidelines (Boumaza et al., 2021; World Health Organization, 2006).

Similarly, for zinc (Zn), its content in the raw sample (220 $mg.kg^{-1}$) exceeded the limit set by the EU (200 $mg.kg^{-1}$) (FAOLEX, s. d.), but it decreased after desliming (180 $mg.kg^{-1}$), falling within the acceptable range (25-200 $mg.kg^{-1}$). Regarding cadmium (Cd), its content in both samples exceeds the EU limit (1 - 3 $mg.kg^{-1}$) (El-Mofty et al., 2018; Friberg et al., 1992). The concentrations of Cu, with an EU soil limit of 50–140 $mg.kg^{-1}$, and As, with a WHO guideline value of 10 $mg.kg^{-1}$, are 8–6 $mg.kg^{-1}$ and 6–5.5 $mg.kg^{-1}$ respectively, indicating that both elements remain well below their respective permissible thresholds and do not pose a risk to the environment or human health (FAOLEX, s. d.; Sabiha-Javied et al., 2009; World Health Organization, 2006).

3.4. ICP-OES

Table 4 presents the concentration percentages of major elements (%) and trace elements (ppm) in the raw sample and the deslimed sample, as determined by ICP-OES. An increase is observed in the valuable component P_2O_5, which represents apatite (from 23.59% to 27.01%), along with a decrease in elements associated with gangue minerals such as dolomite and silica; MgO decreases from 3.05% to 2.85%, and SiO_2 from 10.95% to 2.30%. These results confirm the findings obtained through chemical analyses.

Trace elements are generally represented by rare earth elements (REEs). Unlike heavy metals, which decrease after desliming, the rare earth elements increase in concentration along with the P_2O_5 content, confirming their association with the crystalline structure of apatite (Linares et al., 2023). The elements with the highest concentrations compared to others are light rare earth elements (LREEs) (Fajber et al., 2011) Ce, La, Y, and Nd with contents in the global sample and after desliming respectively at (253.21 – 275.78), (189.90 – 203.16), (160.10 – 173.39), and (123.97 – 127.33), whereas heavy rare earth elements (HREEs) exhibit lower concentrations.

Table 4. Abundance of major elements and trace elements

Element %	P_2O_5	SiO_2	Al_2O_3	CaO	MgO	Fe_2O_3	MnO	TiO_2	K_2O	Na_2O	CO_2
Raw sample	24.12	8.80	ND	40.04	2.55	0.70	< 0.05	< 0.05	0.15	1.02	10.61
Deslimed sample	27.30	2.40	ND	45.88	2.46	0.30	< 0.05	< 0.05	0.10	1.15	11.32

Element ppm	Sc	Y	La	Ce	Pr	Nd	Sm	Eu	Gd	Tb	Dy	Ho	Er	Tm	Yb	Lu
Raw sample	3.33	160.10	189.90	253.21	32.89	123.97	32.77	5.88	19.98	3.29	18.75	5.95	9.97	ND	7.61	1.18
Deslimed sample	3.41	173.39	203.16	275.78	33.63	127.33	35.77	6.82	21.97	4.02	20.45	6.15	10.85	ND	7.95	1.10

3.5. FTIR analysis

Fig. 5 shows the spectra obtained by Fourier Transform Infrared Spectroscopy (FTIR) for the raw sample (g) and the deslimed sample (d). In spectrum (d), a clear intensification of the PO_4^{3-} band (1050 – 1100 cm^{-1}) is observed, confirming the enrichment in P_2O_5 compared to spectrum (g), which corresponds to the raw sample. Conversely, the decrease in the CO_3^{2-} bands at 1420 cm^{-1} and 875 cm^{-1} in spectrum (d) confirms the selective removal of carbonates, while the reduction of the 800 cm^{-1} band indicates a decrease in silica content. In both spectra, the presence of O – H (3400 – 3500 cm^{-1}) and C–H(2920 – 2850

cm^{-1}) bands can be observed, corresponding respectively to the presence of moisture, hydroxide phases, and organic matter. These results are fully consistent with the chemical analysis and validate the effectiveness of desliming in increasing apatite content and reducing gangue minerals, which are generally concentrated in the finer particle fraction.

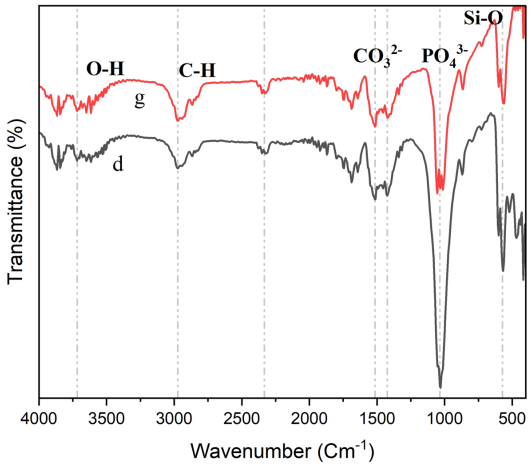

Fig. 5. FTIR spectra of the raw sample (g) and the deslimed sample (d)

3.6. Scanning Electron Microscopy (SEM) observation

The SEM observations of the two samples, before and after desliming, are presented in Fig. 6 and reveal the morphology of the existing minerals. The EDS spectra show that the main elements present in the samples are Ca, O, P, Mg, S, and Na, which is consistent with the chemical analysis results.

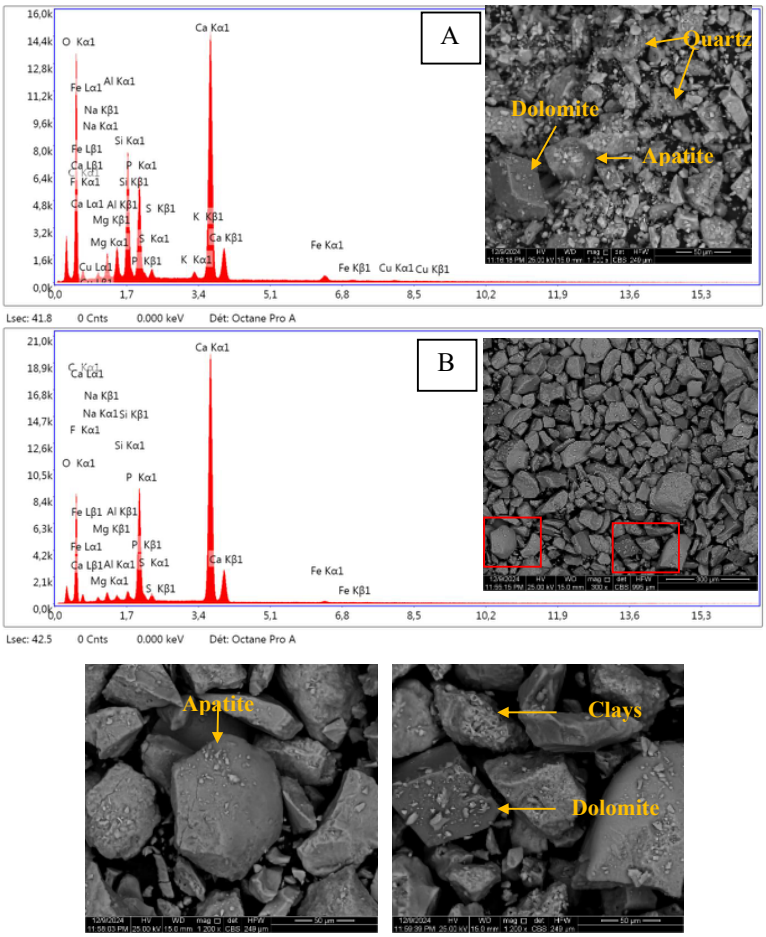

Fig. 6. SEM/EDS of the phosphate sludge sample A - Before desliming, B - After desliming

Consequently, the EDS analysis indicates the presence of major minerals such as apatite, calcite, dolomite, quartz, and other clay minerals. The elemental mapping function of the SEM further confirmed the XRD analysis results. Elemental mapping displays the distribution of each element within the sample. Distinct distributions of Ca, Si, O, Mg, and P key components of calcite, apatite, dolomite, and quartz are observed in both samples. Calcium is a common component of three minerals (calcite, apatite, and dolomite), while oxygen is present in all the minerals, which explains its prominent appearance in the maps (Figs. 7 and 8).

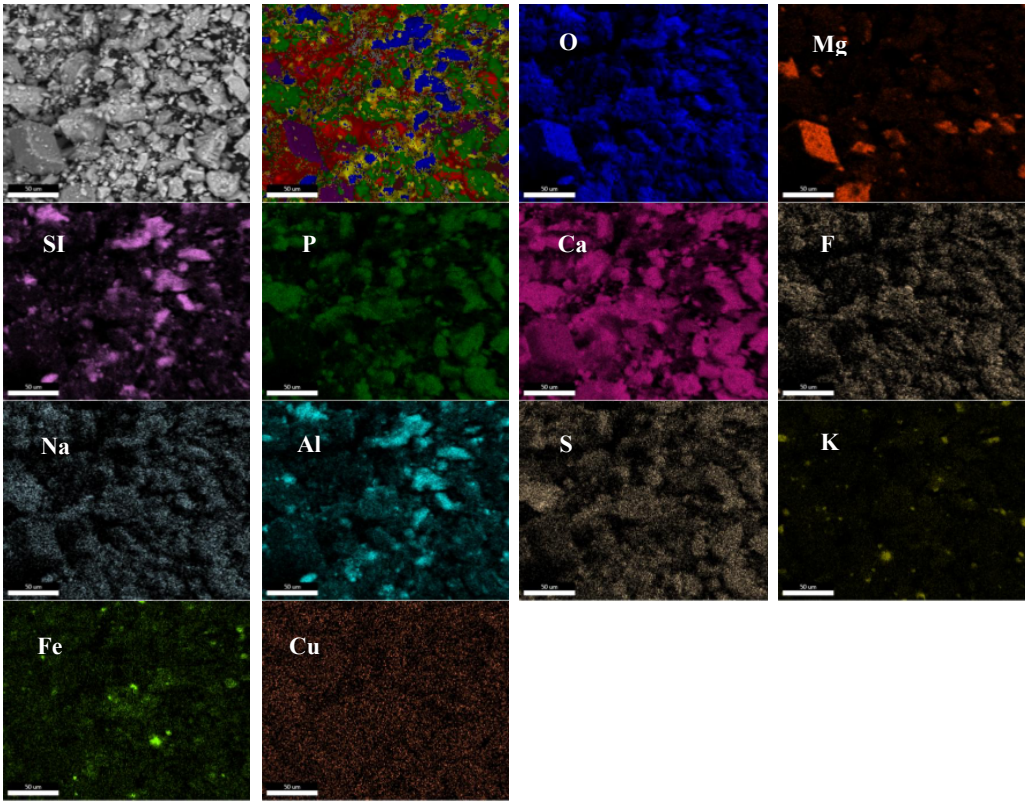

Fig. 7. Elemental mapping of the raw phosphate sludge sample

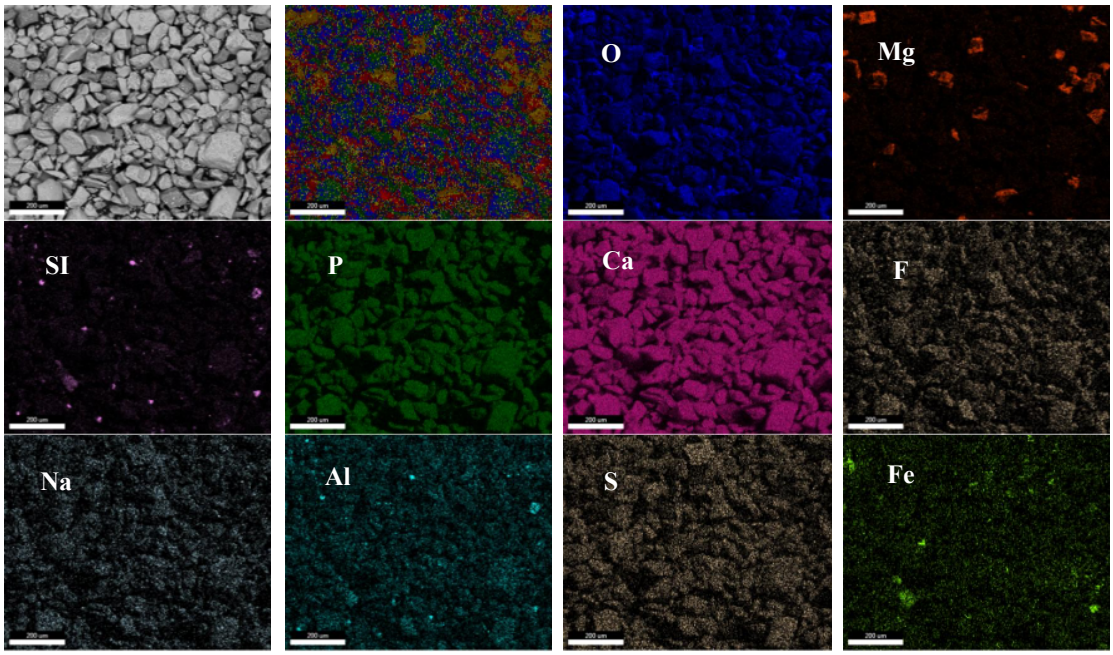

Fig. 8. Elemental mapping of the deslimed phosphate sludge sample

3.7. Micro-XRF

The results obtained by micro-X-ray fluorescence (Fig. 9) include spectra, quantitative data presented in tabular form, and elemental distribution maps. The spectra display characteristic peaks of major elements such as calcium (Ca), silicon (Si), and phosphorus (P), confirming their abundance in the sample. Slight differences were observed between XRF and micro-XRF results. These variations are related to the analytical scale of each method: XRF provides bulk composition, while micro-XRF reflects local heterogeneities of the sample. The latter was mainly used for qualitative confirmation of elemental distribution.

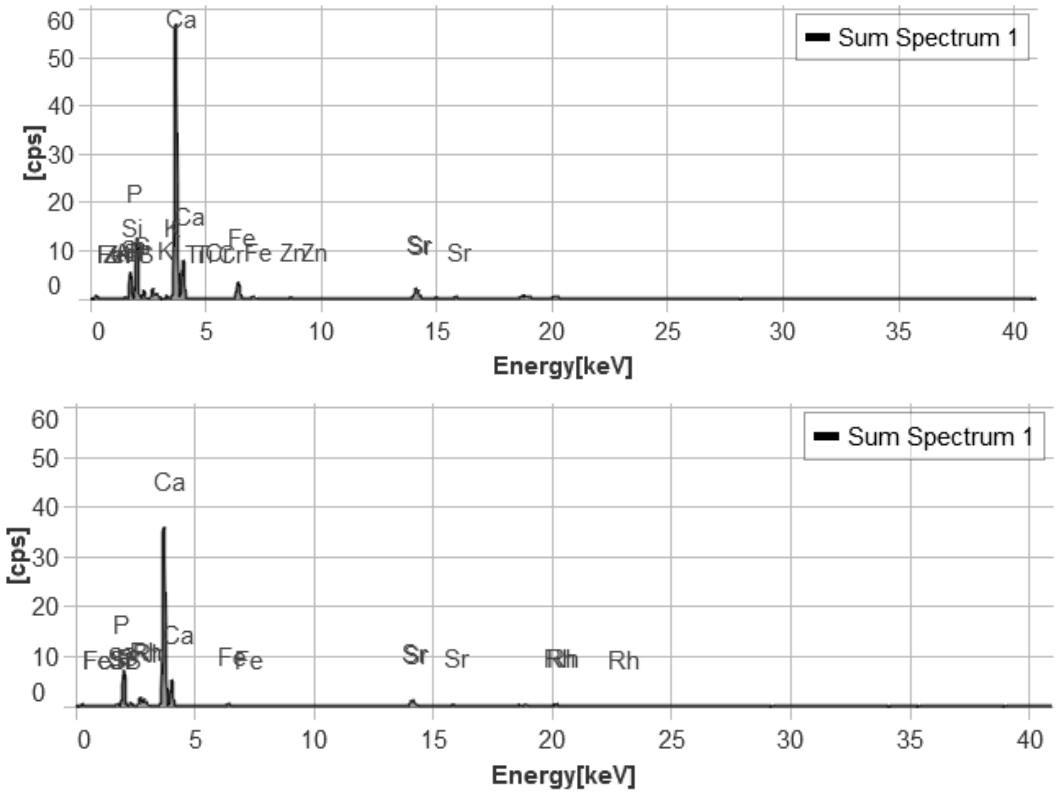

Fig. 9. Elemental spectra obtained by μXRF

Calcium (Ca) and phosphorus (P) show the highest concentrations, with average contents of 69.27% and 14.98%, respectively, in the raw sample, and 80.26% and 14.70%, respectively, after desliming (see Table 5). These results confirm the predominance of carbonate minerals and apatite in the sample. The low concentrations of iron (Fe, 2.25% and 0.87%) and aluminum (Al, 1.79%) indicate the accessory presence of secondary minerals.

Table 5. Results of micro-X-ray fluorescence (μXRF) analysis

Chemical element (%)	Ca	P	Si	S	Fe	Rh	Al	Sr	K	Cr	Ti	Zn
Raw sample	69.27	14.89	8.58	1.32	2.25	-	1.79	0.50	0.86	0.22	0.20	0.10
Deslimed sample	80.26	14.70	1.55	1.07	0.87	0.88	-	0.66	-	-	-	-

The obtained elemental maps show a homogeneous distribution of calcium (Ca) and phosphorus (P), confirming the dominant presence of carbonates and apatite as the main phases. Strontium (Sr) also appears uniformly distributed. In contrast, iron (Fe) and silicon (Si) are observed as weak and localized signals, indicating the presence of accessory inclusions, likely silicate or oxide minerals. Finally, the very low intensity of sulfur (S) and other elements suggests the presence of trace elements, such as heavy metals, in the sample, which is consistent with the results obtained by SEM (Figs. 10 and 11).

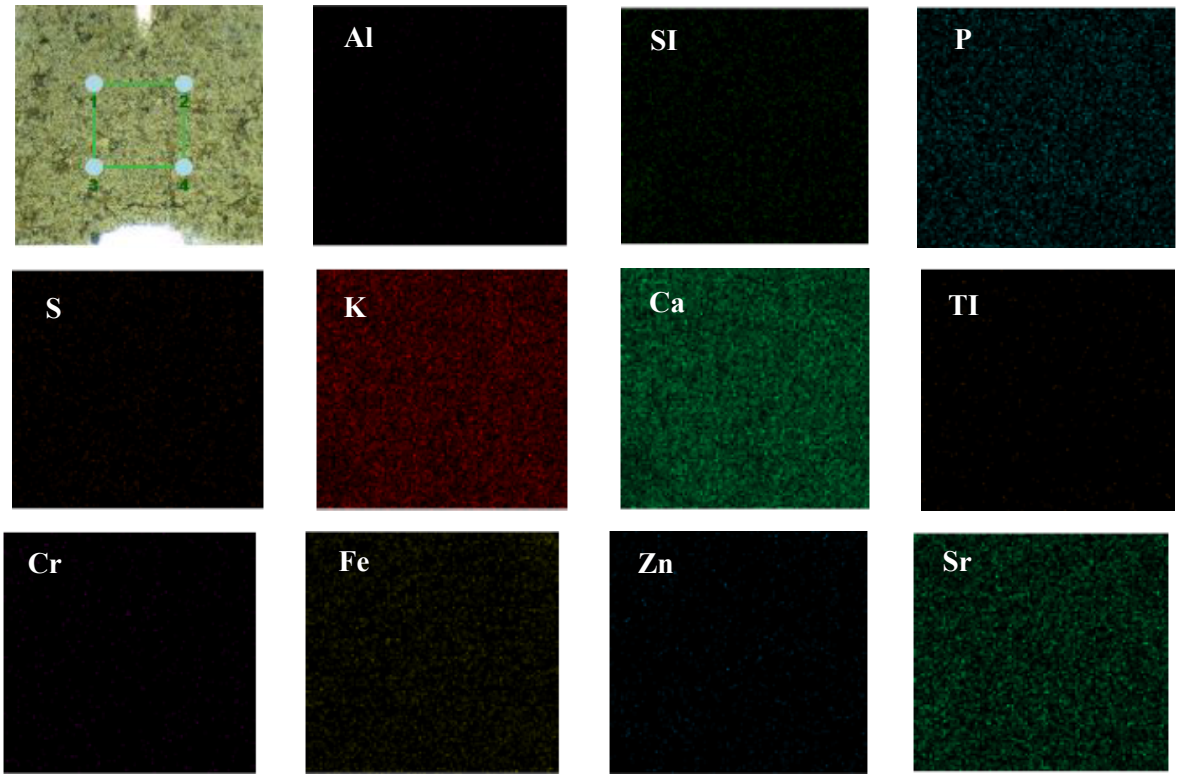

Fig. 10. Elemental mapping by μXRF of the raw sample

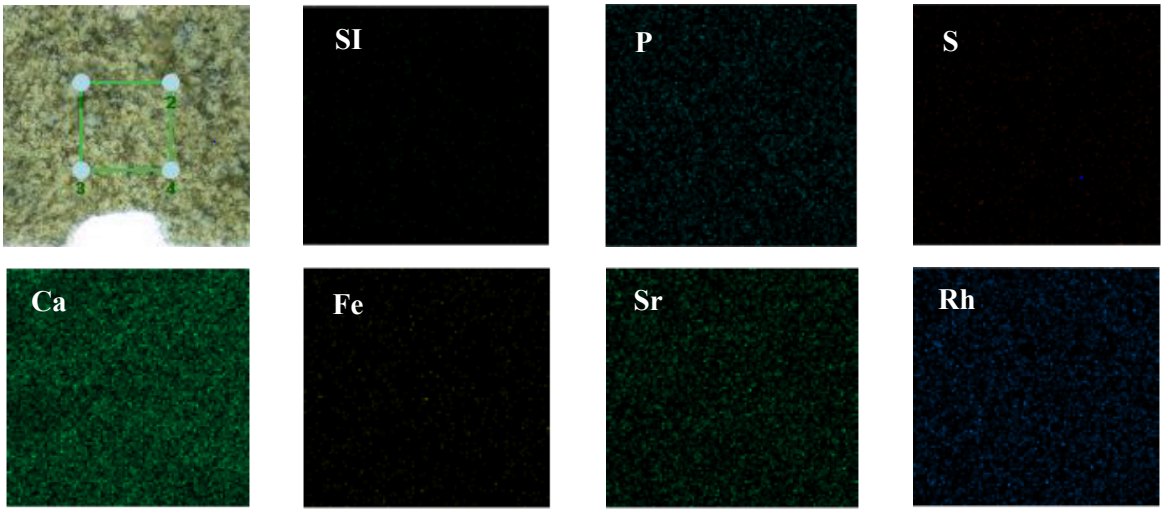

Fig. 11. Elemental mapping by μXRF of the deslimed sample

2.7. Reverse flotation results

The results of the three reverse flotation tests are presented in Table 6. In the first experiment, sulfuric acid was used to depress apatite. The flotation result was suboptimal, though: P_2O_5 in the concentrate declined to 26.69% from a starting 27.01%, and the tailings increased abruptly to 27.47%. This reverse trend shows improper depression of phosphate minerals. A possible explanation for the phenomenon is derived from the acid-induced dissolution of apatite due to the release of Ca^{2+} ions to the pulp. Such ions can interact with HPO_4^{2-} to form surface layers of $CaHPO_4$ (Mohammadkhani et al., 2011) that are capable of altering the surface charge and also hinder effective interaction with depressant molecules. Instead of rendering apatite more hydrophilic, such a change in surface may have involuntarily increased its floatability, resulting in its undesirable transfer to the froth phase (El-Mofty et al., 2018).

In the second test, potassium oleate was employed as a selective collector for carbonates in the first flotation, followed by a cleaning stage without further addition of collector. This practice produced a concentrate with grade P_2O_5 = 29.66% and recovery of 65.84%. The higher grade indicates successful gangue mineral removal, primarily carbonates, though the average recovery indicates that there has been some loss of phosphate. This can be caused by entrainment of fine apatite particles into the froth, lack of depression during cleaning, or ineffective pH control, which affects oleate selectivity. Calcite and apatite flotation performance is highly sensitive to pH due to differences in their isoelectric points, with optimum separation generally occurring at pH 9–10.

The third test blended sodium and potassium tartrate as depressants for phosphates and aluminum sulfate as a pH regulator. This arrangement achieved the maximum separation with a 28.67% concentrate of P_2O_5 and a very high recovery of 97.80%. This is achieved through the combined effect of the reagents: K-Na tartrates adsorb into the surfaces of apatite and complex with Ca^{2+} ions (Mohammadkhani et al., 2011), thereby increasing the hydrophilicity of the surface, and aluminum sulfate reduces free Ca^{2+} concentration by gypsum precipitation ($CaSO_4.2H_2O$). This precipitation changes pulp chemistry, which would be depressing surface contamination of apatite as well as improving gangue floatability. Though no cleaning stage was utilized, the system provided high grade and recovery, illustrating very good selectivity (Mohammadkhani et al., 2011).

Table 6. Flotation experiment results. F: float product; S: sink product; F_1: first float product (rougher flotation); F_2: second float product obtained after cleaner flotation

Experiment	Type	P_2O_5 content (%)	P_2O_5 recovery (%)	MgO content (%)	MgO recovery (%)	SiO_2 content (%)	SiO_2 recovery (%)
01	F	27.47	73.89	2.45	82.19	1.97	33.82
	S	26.69	26.11	1.46	17.81	10.60	66.18
02	F_1	14.21	2.83	4.21	11.40	2.07	3.44
	F_2	26.25	31.33	2.85	46.30	2.19	21.83
	S	29.66	65.84	1.40	42.30	3.22	74.73
03	F	12.34	2.20	4.30	9.92	3.22	6.50
	S	28.67	97.80	2.04	90.80	2.42	93.50

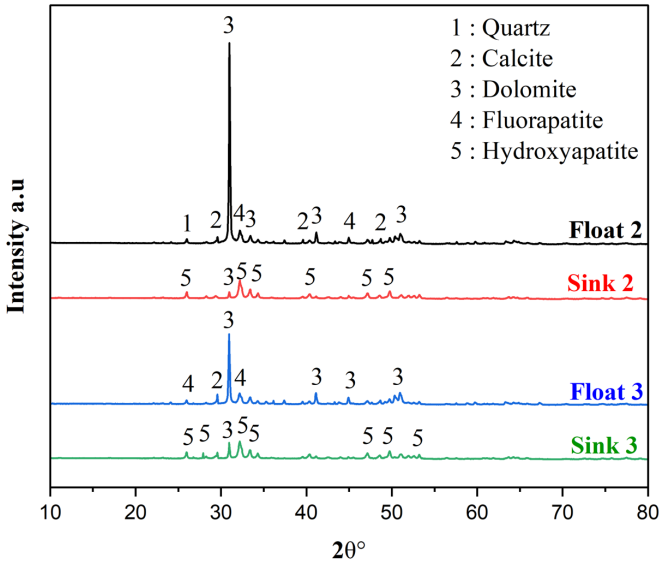

Fig. 12. X-ray diffraction results of the samples from tests 2 and 3

The XRD spectra of the obtained products (Fig. 12) show the absence of hydroxyapatite in the tailings, and its strong presence in the concentrates, which is further confirmed by scanning electron microscopy (SEM) and EDS spectra presented in Fig. 13.

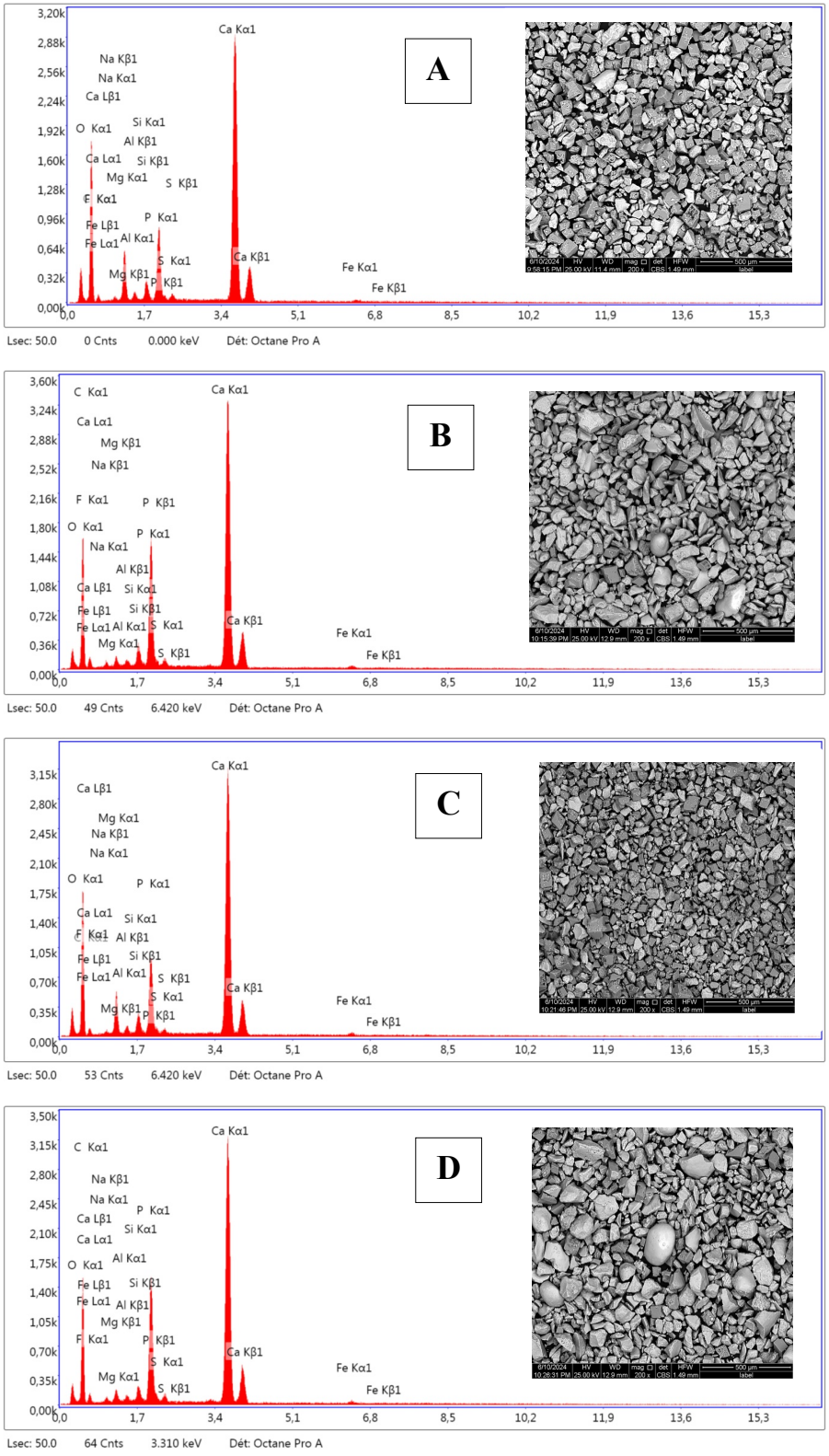

Fig. 13. SEM/EDS analysis of the product obtained from flotation: A- Tailings from Test 01, B- Concentrate from Test 01, C-Tailings from Test 02, D- Concentrate from Test 02

Fig. 14 shows the FTIR spectra of the samples obtained from reverse flotation of phosphate sludge. Spectrum (R) corresponds to the raw feed material, while (F2) and (S2) represent the floated and sunk products from Flotation Test 2, respectively. Finally, (F3) and (S3) correspond to the floated and sunk products from Flotation Test 3, respectively.

The main observations from the FTIR spectra are as follows:

- Band around 1418 cm^{-1} and 872 cm^{-1}: These bands are characteristic of the stretching and bending vibrations of the carbonate group (CO_3^{2-}). They are significantly more intense in the floated products (F_2 and F_3), particularly in F_2, confirming the removal of carbonates after flotation.
- Band around 1052 cm^{-1}: This band is attributed to the asymmetric stretching vibrations of phosphate groups (PO_4^{3-}). It is more prominent in the sunk products (S_2 and S_3), indicating a higher phosphate content in these fractions, especially in S_3, which demonstrates the effectiveness of the depressant (K-Na tartrate) used in the second test.
- Broad bands around 2980-2900 cm^{-1} and 2333 cm^{-1}: These bands may be associated with the presence of organic compounds and CO_2.
- Band around 3712 cm^{-1}: This band is related to the stretching vibrations of hydroxyl groups (OH), typically found in clay minerals or hydrated silicates. It is visible in all samples.

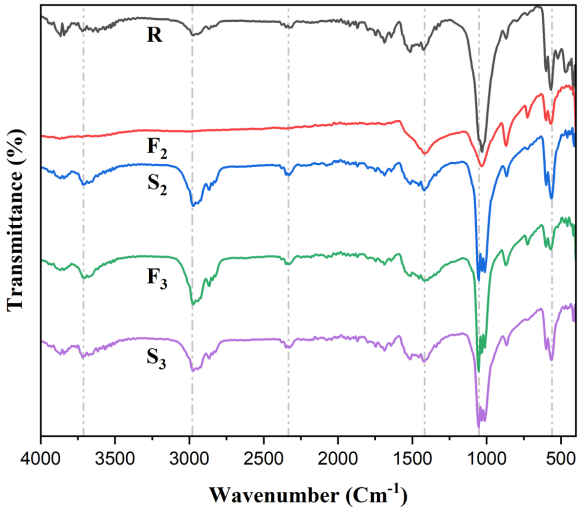

Fig. 14. FTIR spectrum of the product obtained from flotation

Some limitations should be pointed out, in fact, the experiments were conducted at laboratory scale under controlled conditions, which do not fully reflect actual industrial operating environments. Furthermore, the mineralogical complexity and variability of the fine tailings may influence flotation performance, while only a limited number of samples were investigated. The mechanisms of interaction between reagents and mineral surfaces were interpreted mainly based on flotation results, without in-depth surface characterization analyses (such as XPS, zeta potential, or contact angle measurements). Finally, the industrial-scale applicability of the proposed approach was not validated within the scope of this work and requires further investigation.

4. Future perspectives

This study has enabled a good recovery of apatite, which was previously considered as waste, and have helped reduce the environmental impact of fine tailings. For future works, optimization of flotation parameters (pH, type and dosage of reagents, time) looks interesting, followed by advanced analyses (XPS, Raman Spectroscopy, Contact Angle, Zeta Potential) to study the effect of flotation parameters on the quality of the concentrate. We think that micro-flotation tests are also recommended to investigate the interaction between the reagent and the pure mineral. Finally, we also suggest mathematical modelling to predict performance at an industrial scale.

5. Conclusions

This study was conducted using a series of analytical methods on phosphate sludge originating from the phosphate ore processing, as well as its behaviour during flotation experiments. Chemical analyses and ICP-OES were performed according to international standards for phosphate ores. These methods allowed for the quantification of major elements and trace elements (including heavy metals and rare

earth elements) in both the raw and the deslimed sample. X-ray diffraction (XRD) revealed the presence of dominant minerals in the sludge, particularly hydroxyapatite, calcite, dolomite, and quartz. Meanwhile, scanning electron microscopy (SEM) coupled with EDS highlighted the liberation of mineral grains and allowed the identification of their morphologies. FTIR analysis complemented and confirmed the other techniques by identifying functional groups (such as PO_4^{3-} or CO_3^{2-}) and tracking the evolution of mineral phases after treatment, thus validating the effectiveness of the flotation experiments. However, the use of sulfuric acid as apatite depressant in phosphate sludge flotation yielded no significant results due to the presence of Ca^{2+} ions, which prevent the collector from attaching to the mineral surface. Therefore, the proposed solution involved replacing sulfuric acid with K-Na tartrate and adding aluminum sulfate, which reacts with Ca^{2+} ions. The obtained results were promising and encouraging, as confirmed by XRD, SEM/EDS, and FTIR analyses.

Acknowledgments

The authors would like to thank the laboratory team of SOMIPHOS and the LAVAMINE laboratory at Badji Mokhtar University of Annaba for their technical support, as well as the mineral processing laboratory teams at ITU Turkey for their assistance during the experiments.

A part of the results reported in this paper were presented at XX Balkan Mineral Processing Congress BMPC 2026 entitled "Optimization of apatite depression using K–Na Tartrate / $Al_2(SO_4)_3$ in phosphate slimes from Djebel Onk (Algeria)".

References

ABOUZEID, A.-Z. M., 2008. *Physical and thermal treatment of phosphate ores – An overview*. International Journal of Mineral Processing, 85(4), 59-84.

AICHOURI, I., NETTOUR, D., CHAIB, R., DERRARDJIA, N., GHERBI, C., BENSEHAMDI, S., BOUKHAMLA, Y., (2025). *Exhaustive characterization of marble to industrial applications: case of marble from the Filfila deposit (Skikda, northeast Algeria).* Technology audit and production reserves, 5(1 (85)), 12-20.

ALEKSANDROVA, T., ELBENDARI, A., NIKOLAEVA, N., 2022. *Beneficiation of a Low-grade Phosphate Ore Using a Reverse Flotation Technique*. Mineral Processing and Extractive Metallurgy Review, 43(1), 22-27.

AMRANI, M., TAHA, Y., KCHIKACH, A., BENZAAZOUA, M., HAKKOU, R., 2019. *Valorization of Phosphate Mine Waste Rocks as Materials for Road Construction*. Minerals, 9(4), 237.

AVELAR, A. N., BRANDÃO, P. R. G., NEUMANN, R., 2021. *Adsorption of sulfosuccinate collector on apatite and carbonates in a phosphate ore, in the presence of carbon dioxide*. Brazilian Journal of Chemical Engineering, 38(3), 573-583.

BAHHOU, A., TAHA, Y., EL KHESSAIMI, Y., IDRISSI, H., HAKKOU, R., AMALIK, J., BENZAAZOUA, M., 2021. *Use of phosphate mine by-products as supplementary cementitious materials*. Materials Today: Proceedings, 37, 3781-3788.

BOUCIF, R., FILIPPOV, L. O., MAZA, M., BENABDESLAM, N., FOUCAUD, Y., MARIN, J., KORBEL, C., DEMEUSY, B., DIOT, F., BOUZIDI, N., 2024. *Optimizing liberation of phosphate ore through high voltage pulse fragmentation*. Powder Technology, 437, 119549.

BOUJLEL, H., DALDOUL, G., TLIL, H., SOUISSI, R., CHEBBI, N., FATTAH, N., SOUISSI, F., 2018. *The Beneficiation Processes of Low-Grade Sedimentary Phosphates of Tozeur-Nefta Deposit (Gafsa-Metlaoui Basin : South of Tunisia)*. Minerals, 9(1), 2.

BOUMAZA, B., KECHICHED, R., CHEKUSHINA, T. V., 2021. *Trace metal elements in phosphate rock wastes from the Djebel Onk mining area (Tébessa, eastern Algeria) : A geochemical study and environmental implications*. Applied Geochemistry, 127, 104910.

CROZIER, R. D., 1992. Flotatio*n theory, reagents and ore testing*.

Faolex. (s. d.). Directive 86/278/CEE du Conseil relative à la protection de l'environnement, et notamment des sols, lors de l'utilisation des boues d'épuration en agriculture. https://faolex.fao.org /

DERRARDJIA, N., NETTOUR, D., CHETTIBI, M., CHAIB, R., BOUKHAMLA, Y., BENSEHAMDI, S., (2025). *Characterization and development of beneficiation prospects of sedimentary phosphate ore from the Kef Essenoun deposit (Algeria)* by reverse flotation. Technology audit and production reserves, 4(3 (84)), 32-38.

DONG, L., WEI, Q., JIAO, F., QIN, W., 2021. *Utilization of polyepoxysuccinic acid as the green selective depressant for the clean flotation of phosphate ores*. Journal of Cleaner Production, 282, 124532.

EL MACHI, A., MABROUM, S., TAHA, Y., TAGNIT-HAMOU, A., BENZAAZOUA, M., HAKKOU, R., 2021. *Use of flint from phosphate mine waste rocks as an alternative aggregate for concrete*. Construction and Building Materials, 271, 121886.

EL-MOFTY, S. E., EL-MIDANY, A. A., 2018. *Role of calcium ions and their interaction with depressants in phosphate flotation*. Chemical Papers, 72(10), 2641-2646.

ESKANLOU, A., ARNOLD, B. J., FOUCAUD, Y., BADAWI, M., DZADE, N. Y., 2024. *Optimizing flotation separation of fluorapatite from Florida waste clay using a multiscale approach*. Applied Surface Science, 662, 160067.

ETTOUMI, M., JOUINI, M., NECULITA, C. M., BOUHLEL, S., COUDERT, L., TAHA, Y., BENZAAZOUA, M., 2021. *Characterization of phosphate processing sludge from Tunisian mining basin and its potential valorization in fired bricks making*. Journal of Cleaner Production, 284, 124750.

FAJBER, R., SIMANDL, G. J., 2011. *Evaluation of Rare Earth Element-enriched Sedimentary Phosphate Deposits Using Portable X-ray Fluorescence (XRF) Instruments*. Geological Fieldwork, 2012-1.

FRIBERG, L., 1992. *International Program on Chemical Safety, & Weltgesundheitsorganisation (Éds.)*. Cadmium. World Health Organization.

GE, R., YANG, B., MARTIN, R., LUO, H., HE, D., ARROYO, M. A. C., 2023. *The application of poly (sodium 4-styrene sulfonate) as an efficient dolomite depressant in the direct flotation of apatite from dolomite*. Powder Technology, 425, 118583.

HERNÁINZ, F., CALERO, M., BLÁZQUEZ, G., 2004. *Flotation of low-grade phosphate ore*. Advanced Powder Technology, 15(4), 421-433.

LI, D., ZHU, Y., LEI, D., ZHANG, X., GAO, X., HU, X., & LI, S. (2026). *Simultaneous removal of dolomite and feldspar from apatite by reverse flotation: Special selectivity of mixed anionic/cationic collectors*. Journal of Environmental Chemical Engineering, 121247.

LI, X., LI, Y., XIAO, T., LIU, Y., & LI, R., (2025). *Efficient and safe recovery of phosphorus resources from sewage sludge: A study of two-step thermal treatment and the effect of calcination atmosphere*. Chemical Engineering Journal, 166400.

LINARES, E., VELASQUEZ, G., MANRIQUE, J., MONSALVE, J., LO MONACO, S., SHUMLYANSKYY, L., 2023. *REE + Y signatures of the Navay phosphate deposit, SW Venezuela : Seawater paleoredox conditions and diagenetic implications*. Journal of South American Earth Sciences, 129, 104532.

LOUTOU, M., TAHA, Y., BENZAAZOUA, M., DAAFI, Y., HAKKOU, R., 2019. *Valorization of clay by-product from moroccan phosphate mines for the production of fired bricks*. Journal of Cleaner Production, 229, 169-179.

MOHAMMADKHANI, M., NOAPARAST, M., SHAFAEI, S. Z., AMINI, A., AMINI, E., ABDOLLAHI, H., 2011. *Double reverse flotation of a very low grade sedimentary phosphate rock, rich in carbonate and silicate*. International Journal of Mineral Processing, 100(3-4), 157-165.

NAGASAWA, M., SEKIZAWA, O., NITTA, K., KASHIWABARA, T., TAKAHASHI, Y., 2023. *Development of High-Energy μ-X-ray Fluorescence and X-ray Absorption Fine Structure for the Distribution and Speciation of Rare Earth Elements in Natural Samples*. Minerals, 13(6), 746

RUAN, Y., HE, D., CHI, R., 2019. *Review on Beneficiation Techniques and Reagents Used for Phosphate Ores*. Minerals, 9(4), 253.

SABIHA-JAVIED, MEHMOOD, T., CHAUDHRY, M. M., TUFAIL, M., IRFAN, N., 2009. *Heavy metal pollution from phosphate rock used for the production of fertilizer in Pakistan*. Microchemical Journal, 91(1), 94-99.

SALHI, R., NETTOUR, D., CHETTIBI, M., GHERBI, C., BENSELHOUB, A., BELLUCCI, S., 2023. *Characterization of phosphate wastes of Djebel Onk mining complex for a sustainable environmental management*. Technology Audit and Production Reserves, 3(3(71)), 11-19.

SIS, H., CHANDER, S., 2003. *Reagents used in the flotation of phosphate ores: A critical review*. Minerals Engineering, 16(7), 577-585.

TAHRI, T., NARSIS, S., BEZZI, N., GRAIRIA, A., BENGHADAB, K. M., BENSELHOUB, A., 2023. Journal of Geology, Geography and Geoecology, 32(1), 178-184.

WORLD HEALTH ORGANIZATION, 2006. *WHO guidelines for the safe use of wastewater excreta and greywater (Vol. 4)*. World Health Organization.

ZEGHINA, S. I., BOUNOUALA, M., CHETTIBI, M., BENSELHOUB, A., 2020. *Development of new composite cement based on waste rocks from Djebel Onk phosphate deposit (Tebessa-Algeria)*. Naukovyi Visnyk Natsionalnoho Hirnychoho Universytetu, 2, 107-111.